Theoretical investigation of superconductivity mechanism in the filled skutterudites YRu_4P_{12}, YOs_4P_{12}, $LaOs_4P_{12}$ and $LaOs_4As_{12}$

H. Y. Uzunok[1,2], H. M. Tütüncü[1,2],Ertuğrul Karaca[1], G. P. Srivastava[3]

[1] *Sakarya Üniversitesi, BIMAYAM Biyomedikal,*

Manyetik ve Yarıiletken Malzemeler Araştırma Merkezi, 54187, Adapazarı, Turkey

[2] *Sakarya Üniversitesi, Fen-Edebiyat Fakültesi,*

Fizik Bölümü, 54187, Adapazarı, Turkey and

[3] *School of Physics, University of Exeter,*

Stocker Road, Exeter EX4 4QL, UK

(Dated: June 20, 2018)

Abstract

We have investigated the structural, electronic, phonon and electron-phonon interaction properties of the filled skutterudites YRu_4P_{12}, YOs_4P_{12}, $LaOs_4P_{12}$ and $LaOs_4As_{12}$ by utilizing the generalized gradient approximation of the density functional theory. It is found that the electronic states close to the Fermi energy are heavily contributed by the transition metal and pnictogen atoms, while the contribution of the filler atom (Y or La) to the occupied bands is negligible. Our electron-phonon calculations suggest that all these filled skutterudites are conventional phonon-mediated superconductors. The superconducting critical temperature is found to be 7.73, 2.67, 2.03 and 3.2 for YRu_4P_{12}, YOs_4P_{12}, $LaOs_4P_{12}$ and $LaOs_4As_{12}$, respectively. These values are in good agreement with experimentally reported values of 8.5, 2.8, 2.0 and 3.2 K, respectively.

PACS numbers: 63.20.kd, 71.15.Mb, 71.20.Lp, 74.25.Kc

I. INTRODUCTION

Filled skutterudite pnictides with the general formula LnT_4X_{12} (Ln = Lanthanide, T = Transition metal, X = Pnictogen) have received great attention since they exhibit a variety of individual properties, such as semiconducting [1–4], metal-insulator transition [5–8], different magnetic ordering [9–14], good thermoelectricity [15–18], heavy fermion behavior [19, 20] and topological insulator behavior [21, 22]. Furthermore, the La-based skutterudite compounds have received special interest due to their superconducting properties [23–29]. In particular, $LaOs_4P_{12}$ and $LaOs_4As_{12}$ exhibit superconductivity below 2.0 and 3.2 K, respectively [23, 25]. Matsuhira and co-workers [24] reported the specific heat measurement of $LaOs_4P_{12}$ down to 1.8 K. In this experimental work [24], the electronic specific heat coefficient γ of this superconductor is determined to be 21.6 mJ/(mol K^2). Iwahashi and co-workers [25] reported the Haas-van Alphen effect in $LaOs_4P_{12}$ and found multiply-connected and nearly spherical Fermi surfaces with cyclotron effective mass of 1.1-4.7 m_o. Recently, the specific heat measurement of $LaOs_4As_{12}$ has been made by Juraszek and co-workers [28]. This experimental work [28] reveals that a moderate size of specific heat jump signals a weak electron-phonon coupling in this La-based skutterudite compound.

In addition to La-based skutterudite superconductors, Y-based skutterudite superconductors [30–32] have been reported. Electrical resistivity of YOs_4P_{12} [31] displays a superconducting transition at around 3 K which is higher than the corresponding value for $LaOs_4P_{12}$. Electrical and magnetic properties of YRu_4P_{12} have been investigated at low temperatures in the experimental work of Shirotani and co-workers [32]. This experimental work [32] indicates that YRu_4P_{12} displays the superconducting transition (T_c) at around 8.5 K which is much higher than the T_c of YOs_4P_{12}. This filled skutterudite possesses the highest T_c among the Y-based skutterudites [30–32]. By use of synchrotron radiation [33], powder x-ray diffraction of the superconducting skuttetudites YT_4P_{12} (T = Fe, Ru and Os) has been studied at high pressures. Using these results, their bulk modulus have been obtained from the volume versus pressure curves fitted by a Birch equation of state [33]. In 2015, Kawamura and co-workers [34] studied the magnetization on YOs_4P_{12} under pressure up to ~ 4 GPa. Their experimental work reveals that superconductivity in this superconductor can be explained by using the Bardeen-Cooper-Schrieffer (BCS) theory with a negative pressure dependence of T_c (dT_c/dP) due to the stiffness of lattice. This group reported a

similar observation [34] for $LaOs_4P_{12}$.

Although several experimental works exist on the physical properties of YRu_4P_{12}, YOs_4As_{12}, $LaOs_4P_{12}$ and $LaOs_4As_{12}$, theoretical works on these filled skutterudites are certainly not enough to explain the source of superconductivity in them. The full potential linearized augmented plane wave (FLAPW) calculation [35] has been made for the determination of electronic band structure of $LaOs_4As_{12}$ which exhibits metallic character with at least one band passing over the Fermi level. The electronic structure of $LaOs_4P_{12}$ is reported by using the FLAPW method within the local density approximation (LDA) [36]. This theoretical study reveals metallic character of this compound since two electronic bands pass over the Fermi level. An *ab initio* work [37] confirms the dynamical stability of $LaOs_4As_{12}$ because its phonon spectrum does not contain any unstable phonon branches. However, the physical properties of YRu_4P_{12} and YOs_4As_{12} are lacking from the literature. Only, the value of the electronic density of states at the Fermi level for YRu_4P_{12} has been reported to be 5.74 states/eV by the full-potential linearized augmented-plane-wave (FLAPW) calculation of Cheng and co-workers [38]. Furthermore, the electron-phonon interaction properties of all these filled skutterudites have not yet been investigated. This is the most essential part of the BCS superconductivity and thus must be investigated along with the structural, electronic and lattice dynamical properties.

The goal of this work is to make *ab initio* pseudopotential calculations of the structural, electronic, phonon and electron-phonon interaction properties of the filled skutterudites YRu_4P_{12}, YOs_4P_{12}, $LaOs_4P_{12}$ and $LaOs_4As_{12}$ by using a generalized gradient approximation of the density functional theory and a density functional linear response method [39]. The Migdal-Eliashberg approach [40–42] have been applied to investigate electron-phonon interaction. The calculated superconducting transition temperature values T_c are compared favourably with experimentally reported values [23, 25, 34].

II. METHOD

All our calculations have been performed by utilizing the density functional theory (DFT) as implemented in Quantum-Espresso code [39]. Electron-ion interactions are included in the form of norm-conserving pseudo-potentials [43]. Electron-electron exchange and correlation terms have been included within the generalized gradient approximation (GGA) utilizing

the Perdew-Burke-Ernzhof functional [44]. The energy cutoff of the plane wave basis set is chosen as 60 Ry. Self consistent solutions of the Kohn-Sham equations [45] are obtained by employing Monkhorst-Pack special $\boldsymbol{k}$ points [46]: a (8×8×8) mesh is used for the calculation of structural properties, and a (24×24×24) mesh is used for the band structure calculations.

The lattice dynamical calculations have been performed by using the density functional perturbation theory within the linear response approach [39]. As phonon calculations need much more time than electronic calculations, eight dynamical matrices on the (4×4×4) Monkhorst-Pack grid have been used for the computation of real-space force constants. These are then Fourier transformed to determine phonon dispersion relations for any chosen $\boldsymbol{q}$ point.

Within the Migdal-Eliashberg approach [40–42] the phonon linewidth $\gamma_{\boldsymbol{q}j}$ can be given as

$$\gamma_{\mathbf{q}j} = 2\pi\omega_{\mathbf{q}j} \sum_{\mathbf{k}nm} |g^{\mathbf{q}j}_{(\mathbf{k}+\mathbf{q})m;\mathbf{k}n}|^2 \delta(\varepsilon_{\mathbf{k}n} - \varepsilon_F)\delta(\varepsilon_{(\mathbf{k}+\mathbf{q})m} - \varepsilon_F), \tag{1}$$

where the electron-phonon matrix element $g^{\mathbf{q}j}_{(\mathbf{k}+\mathbf{q})m;\mathbf{k}n}$ is determined self-consistently by the linear response theory [39]. By combining the electronic density of states, phonon density of states, and the electron-phonon matrix elements, we express the Eliashberg spectral function(α^2F(ω)) [39–42], the central quantity of the Migdal-Eliashberg approach, in terms of the phonon linewidth $\gamma_{\boldsymbol{q}j}$ of mode j and wavevector $\boldsymbol{q}$ as

$$\alpha^2 F(\omega) = \frac{1}{2\pi N(E_F)} \sum_{\mathbf{q}j} \frac{\gamma_{\mathbf{q}j}}{\hbar\omega_{\mathbf{q}j}} \delta\left(\omega - \omega_{\mathbf{q}j}\right), \tag{2}$$

where $N(E_F)$ denotes the electronic density of states per atom and spin at the Fermi level. The electron-phonon coupling constant can be defined as:

$$\lambda_{\mathbf{q}j} = \frac{\gamma_{\mathbf{q}j}}{\pi\hbar N(\varepsilon_F)\omega^2_{\mathbf{q}j}}. \tag{3}$$

The average electron-phonon coupling constant λ can be estimated from the summation of $\lambda_{\boldsymbol{q}j}$ over all phonon modes ($\boldsymbol{q}$j) in the irreducible part of the Brillouin zone (IBZ),

$$\lambda = \sum_{\boldsymbol{q}j} \lambda_{\boldsymbol{q}j} W(\boldsymbol{q}). \tag{4}$$

where W($\boldsymbol{q}$) denotes the weight of the $\boldsymbol{q}^{\text{th}}$ sampling point. The logarithmically averaged phonon frequency $\omega_{\ln}$ is defined as [39–42]:

$$\omega_{\ln} = \exp\left(\frac{1}{\lambda}\sum_{\boldsymbol{q}j} \lambda_{\boldsymbol{q}j} \ln\omega_{\boldsymbol{q}j}\right). \tag{5}$$

The relation between the superconducting transition temperature T_c and the average electron-phonon coupling strength λ can be defined by the Allen-Dynes modified McMillan formula [42]:

$$T_c = \frac{\omega_{\ln}}{1.2}\exp\left(-\frac{1.04(1+\lambda)}{\lambda-\mu^*(1+0.62\lambda)}\right), \tag{6}$$

where the screened Coulomb repulsion μ^* is chosen to be 0.13 for all the studied compounds. It is worth mentioning that a denser (24×24×24) $\boldsymbol{k}$ mesh was utilized for the electron-phonon coupling calculations, which require more attentive treatment of the Fermi energy. Finally, the value of electronic specific heat coefficient (γ) can be defined as:

$$\gamma = \frac{1}{3}\pi^2 k_B^2 N(E_F)(1+\lambda). \tag{7}$$

III. STRUCTURAL AND ELECTRONIC PROPERTIES

All the compounds studied here adopt the $CoAs_3$ type skutterudite structure filled by Ln atoms (La or Y) with one formula unit per primitive cell. Thus, there are seventeen atoms of three types in the primitive unit cell: one Ln atom in the (2a) position (0, 0, 0), four T (Ru or Os) atoms located at the (8c) positions (1/4, 1/4, 1/4), and twelve X (P or As) atoms at the (24g) positions (0, y, z). The y and z are inner coordinates which designate the relative positions of X atoms in the [T_4X_{12}] polyanion. Thus, the structure of these filled skutterudites is constituted by one lattice parameter (a) and two inner coordinates (y and z). The structure is shown in Fig. 1. Here Y (or La) atoms are located at the corner (0 0 0) and centre (1/2 1/2 1/2) of a cube, while the transition metal atoms are in a distorted octahedral environment of six pnictogen (P or As) atoms [Husein, please see if this sentence reads ok].

Total energy calculations were fitted to the Murnaghan equation of state [47] to obtain the ground state properties such as the equilibrium lattice constant (a), the bulk modulus (B) and its pressure derivative (B$'$). Tab. I presents the determined values of the equilibrium lattice constant (a), the equilibrium primitive unit cell volume (V), inner coordinates (y and z), the bulk modulus (B) and its pressure derivative (B$'$) for all the studied filled skutterudite compounds, as well as, available experimental [25, 33] and theoretical [35, 37] results. In general, our results for the ground state properties are in gratifying accordance with available experimental [25, 33] and theoretical [35, 37] results. In particular, the calculated lattice

constants deviate from their experimental ones [25, 33] by 0.7%, 0.9%, 1.3%, 1.8% for YRu_4P_{12}, YOs_4P_{12}, $LaOs_4P_{12}$, and $LaOs_4As_{12}$, respectively.

Fig. 2 (a) displays the calculated electronic band structure of YRu_4P_{12} along the high symmetry lines in the Brillouin zone of the body-centered cubic lattice. This diagram confirms the metallic character of this filled skutterudite since at least one band crosses the Fermi level. The most gripping feature in this electronic structure is the existence of an almost flat band overlapping with [shall we change 'overlapping with ' to 'in very close proximity of'?] the Fermi level along the N-P symmetry direction. This flat band gives rise to a strong peak at the Fermi level, which may be crucial for superconductivity in this filled skutterudite compound since Cooper pairs in the BCS theory are constituted by electrons having energies close to the Fermi level. A similar observation was also made for borocarbide superconductors [48]. The atom- and symmetry-projected density of states (DOS) for YRu_4P_{12} are also displayed in the Fig. 2(a) to clarify the characters of the bands. At first glance, the partial DOS of Ru and P are substantially distributed in the energy range below and above the Fermi level. However, the partial DOS of Y is disturbed nearly above [shall we clarify the meaning of 'nealy above' ?] the Fermi level. This result is totally expected because Y element is in the form of cation Y^{3+} and behaves like an electron donor. This event signals the picture of a charge transfer from the Y atom to the $[Ru_4P_{12}]$ polyanion. As a consequence, the states close to the Fermi level consist of P p and Ru d orbitals, whereas the contribution from Y orbitals to these states is negligible. The DOS features in the energy window from -14.4 to -12.4 eV, from -11.7 to -9.9 eV and -8.9 to -7.5 eV below the Fermi level are composed of P 3s states. The important valence band region extends from -6.5 eV to the Fermi level. In this region, there is a high degree of hybridization of Ru d states with P p states, which indicates a strong covalent bond between these atoms. This strong bond between these atoms is due to the similarity of their electronegativities. As it is expected from the electronic structure of this filled skutterudite, the Fermi level lies at the top of a sharp peak. The DOS at the Fermi level ($N(E_F)$) for this filled skutterudite amounts to 5.51 States/eV, which is slightly smaller than 5.74 States/eV reported from the FLAPW calculations. Y, Ru and P elements contribute to the value of ($N(E_F)$) by around 1%, 31% and 68%. These results confirm that the contribution of Y to the valence bands is quite small and featureless. The only role Y atom plays is to stabilize the Ru_4P_{12} skutterudite structure. Therefore, Y does not participate in the conductivity of YRu_4P_{12}. However, Ru

4d and P 3p states alone contribute to N(E_F) up to 21% and 55%, respectively. In the light of these results, we can suggest that Ru d and P p states dominate the conductivity of this filled skutterudite. It is worth to note that a similar observation has been made for $LaRu_4P_{12}$ in our previous *ab initio* calculations [29].

Fig. 2 (b) presents the electronic band structure and electronic DOS for YOs_4P_{12}. These look similar to those of YRu_4P_{12} displayed in Fig. 2 (a). This is not surprising since both superconductors are isostructural and isoelectronic to each other. The DOS at the Fermi level for YOs_4P_{12} is computed to be 5.28 State/eV which is slightly smaller than that of YRu_4P_{12}. Again the contribution of Y electronic states to N(E_F) is insignificant, while Os d and P p states contribute up to approximately 26% and 50%, respectively. Although the electronic properties of YRu_4P_{12} and YOs_4P_{12} are similar to each other, the reported T_c of YRu_4P_{12} is much higher than that of YOs_4P_{12}. This observation indicates that the large difference in their T_c values can not be explained by their electronic properties. Thus, phonon and electron-phonon interaction properties of these filled skutterudites must be searched and presented in detail.

The calculated energy band structures and density of states for La-based filled skutterudites are illustrated in Fig. 3. The energy band structures of both skutterudites exhibit metallic character. For both systems, low-lying states arise from the s states of the pnictogen atom. The main valence band region of both skutterudites consists of a mixed character with the hybridized transition metal d and pnictogen p states, which is indicative of the T–X covalent interaction. The states close to the Fermi level for both compounds are mainly dominated by the states of $[T_4X_{12}]$ polyanion. The contributions from La to the occupied bands of both skutterudites are quite small; that is, lanthanum is available in the both skutterudites as the La^{3+} ion and is an electron donor. At the Fermi level, the DOS values are 5.95 and 9.27 states/eV for $LaOs_4P_{12}$ and $LaOs_4As_{12}$, respectively. The larger value of N(E_F) for $LaOs_4As_{12}$ is consistent with its main valence band being narrower by about 1 eV than that of $LaOs_4P_{12}$. The maximum contribution to N(E_F) for both La-filled skutterudites comes from the pnictogen p states with smaller but considerable contribution from transition metal d states: approximately 62% from pnictogen p states and 37% from transition metal d states. Clearly, it is expected that these states will play dominant role in electron-phonon interaction properties of these filled skutterudites. This will be discussed in the following subsection.

The calculated Fermi surfaces of the studied compounds are presented in Fig. 4. The Fermi surface topology for $LaOs_4P_{12}$ is in good agreement with the previous study of Harima and co-worker [36]. Also, the Fermi surface topology of YOs_4P_{12} and $LaOs_4As_{12}$ compounds is similar to that of $LaOs_4P_{12}$. [I do not understand the following sentences. Please rewrite these clearly and carefully. For example, what do you mean when you talk about the 9th band at the Gamma point, etc.] At Γ point, the 9th band of $LaOs_4P_{12}$ and YOs_4P_{12} crosses the Fermi level and forms a nearly perfect spherical Fermi surface sheet along the <100> direction. A similar observation is made for the 11th band of $LaOs_4As_{12}$ compound. On the other hand, this surface is absent in YRu_4P_{12} as the 9th band of this compound does not cross the Fermi level. The 10th band of YRu_4P_{12}, YOs_4P_{12} and $LaOs_4P_{12}$ forms a cubic shaped sheet that is centered at the Γ point. This sheet also connects with the other Fermi surfaces which are centered at the N and P high symmetry points. This observation is also made for the 12th band of $LaOs_4As_{12}$ which forms a more complicated nesting than the other calculated compounds. This could be linked to the smaller separation between the electronic bands crossing the Fermi level for $LaOs_4As_{12}$ than the corresponding separation for the other filled skutterudites studied here.

A. Phonons and electron-phonon interaction

The primitive unit cell of filled skutterudite structure studied in this work consists of 17 atoms, giving rise to 51 phonon branches in all, out of which three are acoustical and the rest of them are optical phonon modes. First, we will discuss the zone-center optical phonon modes of all the studied filled skutterudite compounds since they can be measured by various experimental techniques. According to symmetry analysis, the optical phonon modes at the zone center can be categorized as follows:

$$\Gamma(T_h) = 8T_u(I) + 2A_u(S) + 2E_u(S) + 4T_g(R) + 2E_g(R) + 2A_g(R),$$

with the A, E and T modes being singly, doubly and triply degenerate, respectively. The notations of I, R and S denote infrared active, Raman active and silent modes. The calculated zone-center phonon frequencies for all the considered filled skutterudites are presented in Tab. II together with previous GGA results [37] for $LaOs_4As_{12}$. Unfortunately, we could not find any experimental data for the zone-center phonon frequencies of all the studied com-

pounds. However, the overall agreement between our GGA and previous GGA results [37] for $LaOs_4As_{12}$ is very good.

The calculated phonon spectrum along the high symmetry directions of IBZ, together with the atomic projected phonon density of states, for YRu_4P_{12} are illustrated in Fig. 5 (a). This phonon spectrum has positive phonon frequencies, at any wave vector, suggesting the dynamical stability of this compound in its filled skutterudite structure. The modes can be divided into three apparent regions separated by two forbidden gaps of 0.5 and 0.7 THz due to mass differences between different type of atoms. These three regions extend from 0 to 8.4 THz, from 8.9 to 9.3 THz, and from 10.0 to 14.0 THz. The first region contains 3 acoustical and 21 optical phonon modes. All optical phonon modes in this region exhibit considerable amount of dispersion. The second region includes only 3 optical phonon branches which are less dispersive than the optical phonon branches in the first region. The third region is constituted by 24 optical branches. The characters of these phonon branches can be well explained by discussing the total and partial phonon density of states. At first glance, like the P-related electronic densities, the P-related phonon densities partake in lattice vibrations over the whole range of energies. However, although the mass of Y atom is lighter than that of Ru atom, this filler atom contributes to the low frequency region below 2.3 THz. Above this frequency, the contribution of this filler atom to phonon branches totally disappears. This result reveals that the Y filler atom plays insignificant role in determining the lattice dynamical properties of YRu_4P_{12} as in its electronic properties. In the frequency range from 2.3 to 6.7 THz, a strong overlap between P and Ru vibrations exists. This strong overlap confirms a strong covalent interaction between Ru and P atoms. Above 6.7 THz, the P atom contribution is very dominant since its atomic mass is much lighter than those of the remaining atoms.

The phonon spectrum and phonon density of states for YOs_4P_{12} are presented in Fig. 5 (b). The stability of this filled skutterudite is also confirmed by absence of any imaginary frequency modes in the whole Brillouin zone. The width of this phonon spectrum is about 14.6 THz which is almost equal to that of YRu_4P_{12}. This result is totally expected because the lightest atom for both these filled skutterudites is phosphous. Different from YRu_4P_{12} , the stabilized phonon modes of YOs_4P_{12} are divided into four obvious region separated three phonon band gaps of 1.4, 0.9 and 0.5 THz. This difference is expected to arise from the mass difference between Os and Ru atoms since these filled skutterudites are isostructural

and isoelectronic and local inter-atomic bonding environments are similar. In agreement with YRu_4P_{12}, the contribution of the filler atom to the phonon branches is only present below 2.5 THz. A strong Os–P hybridization exists in the frequency range from 2.5 to 5.2 THz. However, different from YRu_4P_{12}, Os atom remains almost silent in the high frequency domain, which is also related to the heavier mass of Os atom than that of Ru atom.

The phonon spectrum and density of states for $LaOs_4P_{12}$ are displayed in Fig. 6 (a). The phonon spectrum of this filled skutterudite splits into three clear parts with two phonon band gaps of 1.5 and 0.7 THz. These three parts contain 15, 9 and 27 phonon branches, respectively. The DOS features below 3.5 THz include the contributions of all three species. However, the contribution of the filler atom almost vanishes above 4.0 THz. As a consequence, this filler atom only contributes to acoustic and low-frequency optical phonon branches. In the 3.5–5.2 THz range a strong Os–P hybridization is present due to a strong covalent bond between these atoms. However, the contribution of Os almost disappears above the first gap region due to its much heavier mass than the mass of P. While P-related vibrations exist everywhere, they are certainly dominant above the first gap region due to the light mass of P.

The phonon spectrum and density of states for $LaOs_4As_{12}$ are shown in Fig. 6 (b). Different from other filled skutterudites, the 51 phonon branches fill the entire frequency range, leaving no gap in the phonon spectrum of this filled skutterudite. The phonon spectral width of $LaOs_4As_{12}$ is around 8.7 THz which is 5.5 THz smaller than that of $LaOs_4P_{12}$. This can be related to the heavier mass of As atom than that of P atom. The phonon DOS of $LaOs_4As_{12}$ displays a dominance of As atom in the whole frequency range. The filler atom of this compound contributes to lattice vibrations below 3.0 THz while the contribution of Os atom exists up to 7.7 THz. We can conclude that the electronic and vibrational properties of all the considered filled skutterudites are are governed by $[T_4X_{12}]$ polyanion. Therefore, it can be largely expected that the coupled motion of transition metal atom and pnictogen atom will bring about considerable electron-phonon interaction in all the considered filled skutterudites because transition metal d and pnictogen p states dominate density of states at the Fermi level. This will be presented and discussed in the following.

The main objective of this work is to analyze the strength of the electron-phonon interaction in all the considered filled skutterudites in order to identify the source of superconductivity in them. To this end, the Eliashberg spectral function ($\alpha^2F(\omega)$) and the frequency

variation of the average electron-phonon coupling parameter λ for YRu_4P_{12} are presented in Fig. 7 (a). The value of λ amounts to 0.78 which reveals that electron-phonon interaction in this filled skutterudite is of medium strength. It is worth to mention that the vibrational modes between 2.3 and 6.7 THz make a contribute of about 60% towards λ. This large contribution is expected since phonon modes in this region are mainly due to the coupled motion of Ru and P atoms. At this point we remind that the dominant contribution to the density of states at the Fermi level also comes from the Ru d and P p states. Our results suggest that phonons above 6.7 THz contribute about 28% to λ. This large contribution from these phonon modes can be associated with the considerable existence of P p states near the Fermi level.

Fig. 7 (b) displays the Eliashberg spectral function ($\alpha^2F(\omega)$) and the frequency variation of the average electron-phonon coupling parameter λ for YOs_4P_{12}. The value of λ for this filled skutterudite is 0.55 which indicates that electron-phonon interaction in this filled skutterudite is weaker than that in YRu_4P_{12}. As we have mentioned before, a strong Os–P hybridization is present in the frequency range from 2.5 to 5.2 THz. Thus, phonon modes in this region contribute to about about 60% towards λ. Phonon modes above the first gap region contribute about 40% towards λ. This large contribution is expected because these phonon modes are dominated by the vibrations of As atoms which make the largest contribution to the value of $N(E_F)$.

Fig. 8 illustrates the Eliashberg spectral function ($\alpha^2F(\omega)$) and the frequency variation of the average electron-phonon coupling parameter (λ) for La-based filled skutterudites. The value of λ is determined to be 0.49 for $LaOs_4P_{12}$ and 0.59 for $LaOs_4As_{12}$. For $LaOs_4P_{12}$, phonon modes in the first region contribute to about 47% towards λ. It is worth mentioning that these phonon modes are due to the coupled motion of Os and P atoms. As-related phonon modes above the first gap region contribute about 53% towards λ. For $LaOs_4As_{12}$, significant overlap between Os and As vibrations is present below 5.0 THz while phonon modes above this frequency are mainly dominated by the vibrations of As atoms. These phonon modes contribute respectively about 44% and 56% towards λ. This clearly suggests that transition metal and pnictogen-related phonon modes couple strongly with their electrons due to the considerable existence of transition metal d electrons and pnictogen p electrons at the Fermi level.

Finally, the calculated physical quantities [$N(E_F)$, ω_{ln}, λ, γ and T_c] connected to su-

perconductivity in all the studied filled skutterudites are presented in Tab. III. YRu_4P_{12}, YOs_4P_{12}, $LaOs_4P_{12}$ and $LaOs_4As_{12}$ are found to be metallic exhibiting superconductivity below 7.73, 2.67, 2.03 and 3.38 K, respectively. These values are in satisfactory accordance with their measured values of 8.5, 2.8, 2.0 and 3.2 K [23, 25, 34]. The value of γ is found to be 20.88 and 34.7 mJ/(mol K^2) for $LaOs_4P_{12}$ and $LaAs_4P_{12}$ which are comparable with their measured values [24, 26] of 21.6 and 49 mJ/(mol K^2). This table clearly shows that the differences in the T_c values of these filled skutterudites can not be explained by only electronic structure calculations. First, although the $N(E_F)$ values of YRu_4P_{12} and YOs_4P_{12} are very close to each other, the T_c of YRu_4P_{12} is more than two times larger than that of YOs_4P_{12}. Secondly, $LaOs_4As_{12}$ possesses the highest $N(E_F)$ value among all the studied filled skutterudites but its T_c is lower than that of YRu_4P_{12}. However, the value of λ can be used to explain the differences in the T_c values of these filled skutterudites since the value of T_c for these filled skutterudites increases with increase in the value of λ.

IV. SUMMARY

In this work, we have examined the structural, electronic, phonon and electron-phonon interaction properties of the filled skutterudites YRu_4P_{12}, YOs_4P_{12}, $LaOs_4P_{12}$ and $LaOs_4As_{12}$ by utilizing the generalized gradient approximation of the density functional theory. The calculated band structures of these filled skutterudites indicate their metallic character with at least one band crossing the Fermi level. A critical assessment of their electronic DOS reveals that the partial DOS of transition metal and pnictogen are widely scattered in the energy range below and above the Fermi level but the contribution of the filler atom to the valence bands is very small and featureless. As a consequence, the electronic properties of these filled skutterudites are specified by the electronic states of $[T_4X_{12}]$ polyanion, whereas the filler atom stabilizes their crystal structure by giving electrons to $[T_4X_{12}]$ polyanion.

Using our structural and electronic results, the lattice dynamical properties of all the studied filled skutterudites have been investigated by employing a linear response approach based on density functional theory. The calculated zone-center phonon modes for $LaOs_4As_{12}$ are in gratifying accordance with previous theoretical results. Our phonon calculations confirm the dynamical stability of all the studied filled skutterudites because their phonon dispersion curves have real positive frequencies. A critical examination of their phonon DOS

suggests that the lattice dynamical properties of these filled skutterudites are governed by atoms in $[T_4X_{12}]$ polyanion. The phonon spectrum and the electron-phonon matrix elements are used to calculate the Eliashberg spectral function for all the studied compounds. A critical analysis of this spectral function suggests that the motion of filler atoms plays a relatively insignificant role in determining electron-phonon interaction properties of these filled skutterudites. However, phonon modes due to the coupled motion of transition metal and pnictogen atoms are strongly involved in the process of scattering of electrons. The value of average electron-phonon coupling constant is calculated to be 0.78, 0.55, 0.49 and 0.59 for YRu_4P_{12}, YOs_4P_{12}, $LaOs_4P_{12}$ and $LaOs_4As_{12}$, respectively. These results indicate that electron-phonon interaction in YRu_4P_{12} is stronger than that in the remaining filled skutterudites. Finally, our *ab initio* calculations indicate that YRu_4P_{12}, YOs_4P_{12}, $LaOs_4P_{12}$ and $LaOs_4As_{12}$ are all metallic exhibiting superconductivity below 7.73, 2.67, 2.03 and 3.38 K. These T_c values are consistent with their experimentally reported values of 8.5, 2.8, 2.0 and 3.2 K.

ACKNOWLEDGMENTS

[Please change as appropriate.] This work was supported by the Scientific and Technical Research Council of Turkey (TÜBİTAK) (Project Number MFAG-115F135). Some of the calculations for this project were carried out using the computing facilities on the Intel Nehalem (i7) cluster (ceres) in the School of Physics, University of Exeter, United Kingdom.

[1] I. Shirotani, T. Adachi, K. Tachi, S. Todo, K. Nozawa, T. Yagi, and M. Kinoshita, J. Phys. Chem. Solids **57**, 211 (1996).

[2] I. Shirotani, T. Uchiumi, C. Sekine, M. Hori, S. Kimura, N. Hamaya J. Solid State Chem. **142**, 146 (1999).

[3] H. Okamura, R. Kitamura, M. Matsunami, H. Sugawara, H. Harima, H. Sato, T. Moriwaki, Y. Ikemoto, and T. Nanba, J. Phys. Soc. Jpn. **80**, 084718 (2011).

[4] A. Shankar, P. K. Mandal, and B. K. Thapa, J. Mater. Sci. **52**, 1511 (2017).

[5] K. Matsuhira, Y. Hinatsu, C. Sekine, T. Togashi, H. Maki, I. Shirotani, H. Kitazawa, T. Takamasu, and G. Kido, J. Phys. Soc. Jpn. **71**, 237 (2002).

[6] M. Matsunami, L. Chen, H. Okamura, T. Nanba, C. Sekine and, I. Shirotani, J. Magn. Magn. Mater. **272**–**276**, e39 (2004).

[7] H. Hidaka, I. Ando, H. Kotegawa, T. C. Kobayashi, H. Harima, M. Kobayashi, H. Sugawara, and H. Sato, Phys. Rev. B **71**, 073102 (2005).

[8] Y. Imai, K. Sakurazawa, and T. Saso, J. Phys. Soc. Jpn. **75**, 033706 (2006).

[9] M.S. Torikacjvili, J.W. Chen, Y. Dalichaouch, R.P. Guertin, C. McElfresh, M.W. Rossel, M.B. Maple, G.P. Meisner Phys. Rev. B **36**, 8660 (1987).

[10] R. Giri, C. Sekine, Y. Shimaya, I. Shirotani, K. Matsuhira, Y. Doi, Y. Hinatsu, M. Yokoyama, H. Amitsuka Physica B **329**–**333**, 458 (2003).

[11] E. D. Bauer, A. Slembarski, N. A. Frederick, W. M. Yuhasz, M. B. Maple, D. Cao, F. Bridges, G. Giester, P. Rogl, J. Phys.: Condens. Matter **16**, 5095 (2004).

[12] Y. Nakai, K. Ishida, D. Kikuchi, H. Sugawara, H. Sata, J. Phys. Soc. Jpn. **74**, 3370 (2005).

[13] W. M. Yuhasz, N. P. Butch, T. A. Sayles, P.-C. Ho, J. R. Jeffries, T. Yanagisawa, N. A. Frederick, M. B. Maple, Z. Henkie, A. Pietraszko, S. K. McCall, M. W. McElfresh, and M. J. Fluss Phys. Rev. B **73**, 144409 (2006).

[14] S. Tatsuoka, H. Sato, K. Tanaka, M. Ueda, D. Kikuchi, H. Aoki, T. Ikeno, K. Kuwahara, Y. Aoki, H. Sugawara, H. Harima, J. Phys. Soc. Jpn. **77**, 033701 (2008).

[15] A. Watcharapasorn, R.C. Demattei, R.S. Feigelson, T. Caillat, A. Borschcevsky, G.J. Snyder, J.-P. Fleurial, J. Appl. Phys. **86**, 6231 (1999).

[16] C. Sekine, K. Akita, N. Yanase, I. Shirotani, I. Inagawa, C.H. Lee Jpn. J. Appl. Phys. **40**, 3326 (2001).

[17] Y. Qiu, L. Xi, X. Shi, P. Qiu, W. Zhang, L. Chen, J. R. Salvador, J. Y. Cho, J. Yang, Y. Chien, S. Chen, Y. Tang, G. J. Snyder, Adv. Funct. Mater. **23**, 3194 (2013).

[18] X. Shi, J. Yang, L. Wu, J. R. Salvador, C. Zhang, W. L. Villaire, D. Haddad, J. Yang, Y. Zhu, Q. Li, Sci. Rep. **5**, 14641 (2015).

[19] Y. Aoki, T. Namiki, T. M. Matsuda, K. Abe, H. Sugawara, H. Sato, Phys. Rev. B **65**, 064446 2002.

[20] H. Sugawara, T. D. Matsuda, K. Abe, Y. Aoki, H. Sato, S. Nojiri, Y. Inada, R. Settai, and Y. Onuki, Phys. Rev. B **66**, 134411 (2002).

[21] B. Yan, L. Müchler, X.-L. Qi, S.-C. Zhang, C. Felser, Phys. Rev. B **85**, 165125 (2012).

[22] L. Müchler, F. Casper, B. Yan, S. Chadov, C. Felser, Phys. Status Solidi RRL **7**, 91 (2013).

[23] I. Shirotani, K. Ohno, C. Sekine, T. Yagi, T. Kawakami, T. Nakanishi, H. Takahashi, J. Tang, A. Matsushita, and T. Matsumoto, Physica B **2819**–**282**, 1021 (2000).

[24] K. Matsuhira, Y. Doi, M. Wakeshima, Y. Hinatsu, K. Khiou, C. Sekine and I. Shirotani, Physica B **3599**–**361**, 977 (2005).

[25] Y. Iwahashi, H. Sugawara, Ko-ichi Magishi, T. Saito, K. Koyama, R. Settai, Y. Onuki, G. Giester, and P. Rogl, J. Phys. Soc. Jpn. **77**, 219 (2008).

[26] K. Matsuhira, C. Sekine, M. Wakeshima, Y. Hinatsu, T. Namiki, K. Takeda, I. Shirotani, H. Sugawara, D. Kikuchi, and H. Sato, J. Phys. Soc. Jpn. **78**, 124601 (2009).

[27] K. Huang, D. Yazıcı, B. D. White, I. Jeon, A. J. Breindel, N. Pouse, and M. B. Maple Phys. Rev. B **94**, 094501 (2016).

[28] J. Juraszek, Z. Henkie and T. Cichorek, Acta Phys. Pol. A **130**, 597 (2016).

[29] H. M. Tütüncü, Ertuğrul Karaca and G. P. Srivastava, Phys. Rev. B **95**, 214514 (2017).

[30] I. Shirotani, Y. Shimaya, K. Kihou, C. Sekine, N. Takeda, M. Ishikawa, and T. Yagi, J. Phys. Condens. Matter **15**, S2201 (2003).

[31] K. Kihou, I. Shirotani, Y. Shimaya, C. Sekine, and T. Yagi, Mater. Res. Bull. **39**, 317 (2004).

[32] I. Shirotani, N. Araseki, Y. Shimaya, R. Nakata, K. Kihou, C. Sekine and T. Yagi, Journal of Physics: Condensed Matter **17**, 4383 (2005).

[33] J. Hayashi, K. Akahira, K. Matsui, H. Ando, Y. Sugiuchi, K. Takeda, C. Sekine, I. Shirotani, and T. Yagi, J. Phys.: Conf. Ser. **215**, 012142 (2010).

[34] Y. Kawamura, H. Mikage, Yu Qi Chen, J. Hayashi, C. Sekine, H. Gotou, and Z. Hiroi, Physics Procedia **75**, 200 (2015).

[35] D. J. Singh, M. Fornari, J. L. Feldman and I. I. Mazin, "First principles studies of novel thermoelectric materials", Proc. Eighteenth International Conference on Thermoelectrics, IEEE (Baltimore, 1999) pp. 448-450.

[36] H. Harima and K. Takegahara, Physica B **403**, 906 (2008).

[37] M. M. Koza, D. A. Droja, N. T. Akeda, Z. Henkie, and T. C. Ichorek, Journal of the Physical Society of Japan. **82**, 114607 (2013).

[38] J.-G. Cheng, J.-S. Zhou, K. Matsubayashi, P. P. Kong, Y. Kubo, Y. Kawamura, C. Sekine, C. Q. Jin, J. B. Goodenough, and Y. Uwatoko Phys. Rev. B **88**, 024514 (2013).

[39] P. Giannozzi, O. Andreussi, T. Brumme, O. Bunau, M. Buongiorno Nardelli, M. Calandra, R. Car, C. Cavazzoni, D. Ceresoli, M. Cococcioni, N. Colonna, I. Carnimeo, A. Dal Corso, S.

de Gironcoli, P. Delugas, R. A. DiStasio Jr., A. Ferretti, A. Floris, G. Fratesi, G. Fugallo, R. Gebauer, U. Gerstmann, F. Giustino, T. Gorni, J. Jia, M. Kawamura, H-Y. Ko, A. Kokalj, E. Küçükbenli, M. Lazzeri, M. Marsili, N. Marzari, F. Mauri, N. L. Nguyen, H-V. Nguyen, A. Otero-de-la-Roza, L. Paulatto, S. Poncé, D. Rocca, R. Sabatini, B. Santra, M. Schlipf, A. P. Seitsonen, A. Smogunov, I. Timrov, T. Thonhauser, P. Umari, N. Vast, X. Wu and S. Baroni, J. Phys.: Condens. Matter **29**, 465901-1 (2017).

[40] A. B. Migdal, Sov. Phys. JETP **34**, 996 (1958).

[41] G. M. Eliashberg, Zh. Eksp. Teor. Fiz. **38**, 966 (1960) [Sov. Phys. JETP 11, 696 (1960)].

[42] P. B. Allen and R. C. Dynes, Phys. Rev. B **12**, 905 (1975).

[43] R. Stumpf, X. Gonze and M. Scheffler, A List of Separable, Norm-conserving, Ab Initio Pseudopotentials (Fritz-Haber-Institut, Berlin, 1990).

[44] J. P. Perdew, K. Burke, and M. Ernzerhof, Phys. Rev. Lett. **77**, 3865 (1996).

[45] W. Kohn and L. J. Sham, Phys. Rev. **140**, A1133 (1965).

[46] H. J. Monkhorst and J. D. Pack, Phys. Rev. B **13**, 5189 (1976).

[47] Murnaghan F D, Proc. Nat. Acad. Sci. USA **50**, 697 (1944).

[48] H. M. Tütüncü, H. Y. Uzunok, Ertuğrul Karaca, G. P. Srivastava, S. Özer, and Ş. Uğur, Phys. Rev. B **92**, 054510 (2015).

TABLE I: Structural properties of the filled skutterudites YRu_4P_{12}, YOs_4As_{12}, $LaOs_4P_{12}$, $LaOs_4As_{12}$ and their comparison with previous experimental and theoretical results.

Superconductor	$a(\AA)$	V($\AA^3$)	y	z	B(GPa)	$B^{'}$
YRu_4P_{12}	8.085	264.25	0.3575	0.1428	164	4.47
Experimental [33]	8.029	258.87			183	
YOs_4P_{12}	8.136	269.28	0.3570	0.1419	172	4.45
Experimental [33]	8.062	261.99			189	
$LaOs_4P_{12}$	8.193	274.97	0.3590	0.1436	172	4.60
Experimental [25]	8.093	265.03	0.3576	0.1434		
Experimental [33]	8.084	264.14			190	
$LaOs_4As_{12}$	8.706	329.93	0.3489	0.1504	126	5.06
Experimental [33]	8.544	311.86				
LDA [35]			0.3488	0.1502		
GGA [37]	8.637	322.15	0.3481	0.1500	114	

TABLE II: The zone-center phonon frequencies (in THz) of the filled skutterudites YRu_4P_{12}, YOs_4P_{12}, $LaOs_4P_{12}$ and $LaOs_4As_{12}$. Previous GGA results for $LaOs_4As_{12}$ [37] are presented in brackets. The notations I, R and S denote infrared active, Raman active and silent modes.

Mode	YRu_4P_{12}	YOs_4P_{12}	$LaOs_4P_{12}$	$LaOs_4As_{12}$
T_u (I)	2.00	1.79	3.11	2.12 (1.85)
	5.28	4.34	4.59	3.67 (3.57)
	6.24	4.93	4.91	4.06 (4.00)
	7.36	6.89	6.87	4.82 (4.80)
	8.42	7.79	7.79	5.29 (5.20)
	10.23	10.15	9.64	6.26 (6.14)
	11.81	11.57	11.18	6.49 (6.50)
	11.97	11.99	12.39	6.87(7.03)
A_u(S)	4.47	3.16	3.61	2.58 (2.65)
	10.72	11.03	10.59	6.70 (6.83)
E_u(S)	6.20	4.75	4.65	3.84 (3.79)
	11.11	11.28	10.96	7.17 (7.36)
T_g (R)	7.04	7.19	7.64	4.09 (3.96)
	8.89	9.21	9.15	4.74 (4.79)
	10.41	10.95	10.56	6.48 (6.60)
	12.16	12.88	12.48	7.72 (7.89)
E_g (R)	10.32	10.05	10.17	5.52
	12.36	12.52	12.32	6.37
A_g (R)	10.89	11.13	10.57	5.87 (5.40)
	12.43	12.61	12.81	6.49 (6.78)

TABLE III: The calculated values of the physical quantities related to superconductivity in the studied filled skutterudites.

Compound	$N(E_F)$ (States/eV)	ω_{ln} (K)	λ	$\gamma(\frac{mJ}{molK^2})$	T_c (K)
YRu_4P_{12}	5.51	216.97	0.78	23.03	7.73
Experimental [34]					8.5
FLAPW [38]	5.74				
YOs_4As_{12}	5.28	235.41	0.55	19.23	2.67
Experimental [34]					2.8
$LaOs_4P_{12}$	5.95	293.96	0.49	20.88	2.03
Experimental [24]				21.6	1.8
Experimental [25]					2.0
$LaOs_4As_{12}$	9.27	221.81	0.59	34.7	3.38
Experimental [23]					3.2
Experimental [26]				49	

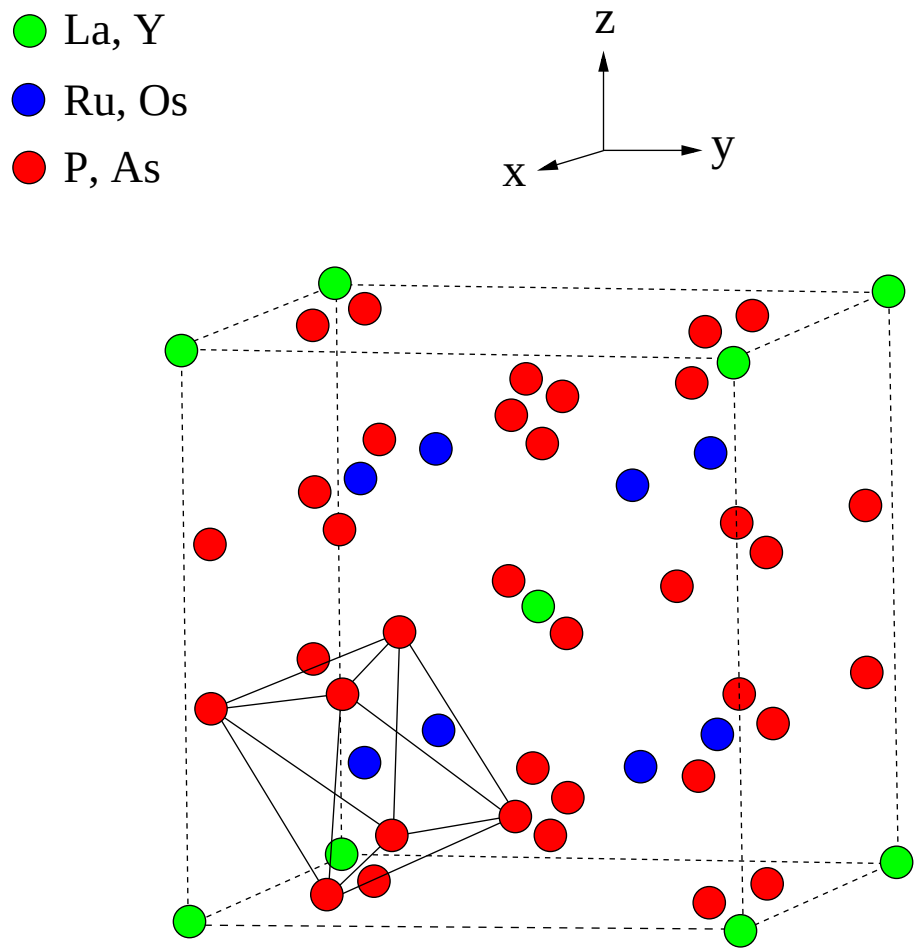

FIG. 1: Crystal structure of the filled skutterudites YRu_4P_{12}, YOs_4P_{12}, $LaOs_4P_{12}$ and $LaOs_4As_{12}$. Y (or La) atoms are located at (000) and (1/2 1/2 1/2) of a cubic structure like bcc while Ru (or Os) atoms sit in the center of a distorted octahedral environment of six P (or As) atoms.

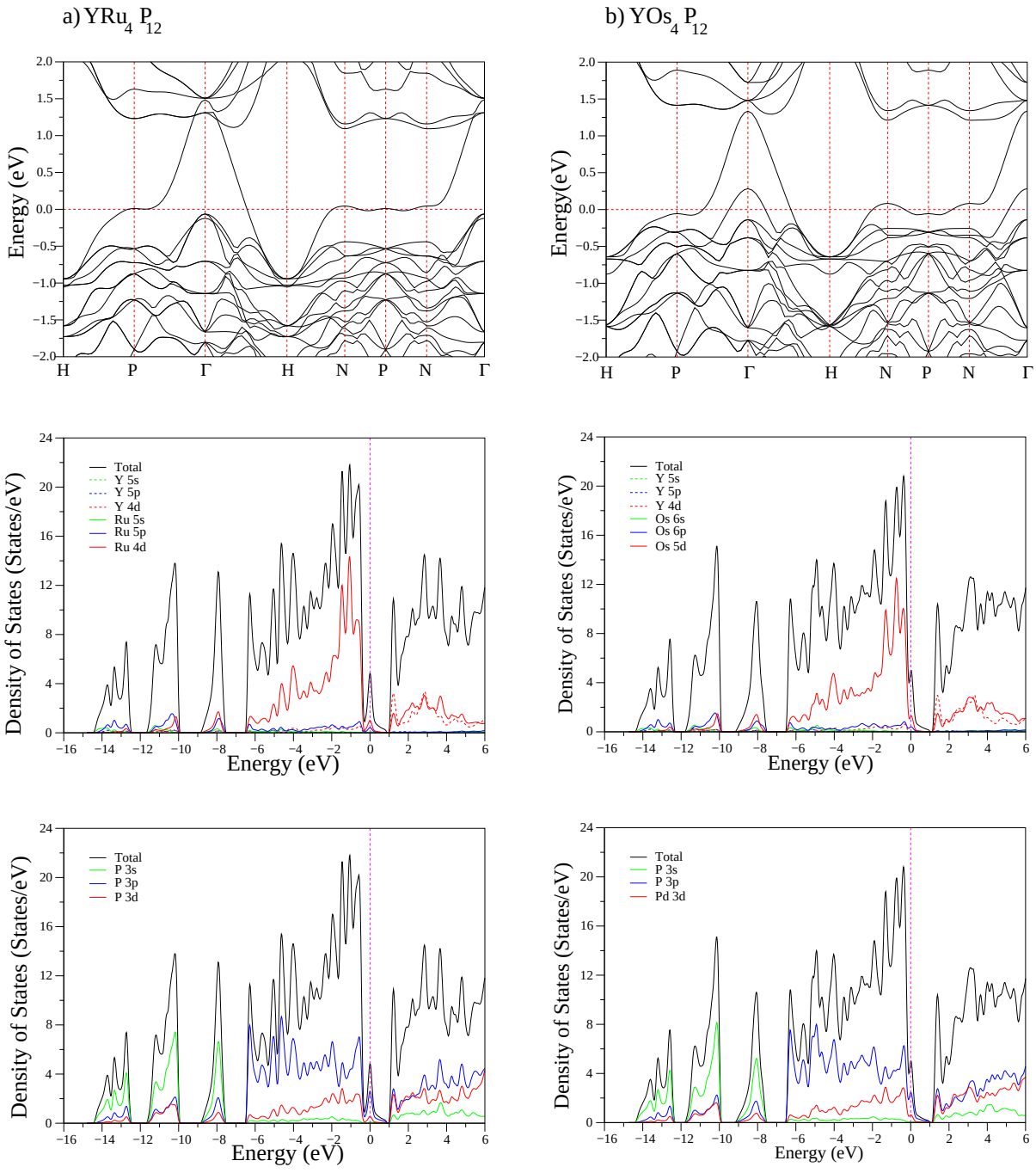

FIG. 2: The electronic band structure and density of states for (a) YRu_4P_{12} and (b) YOs_4P_{12}. The Fermi level corresponds to 0 eV.

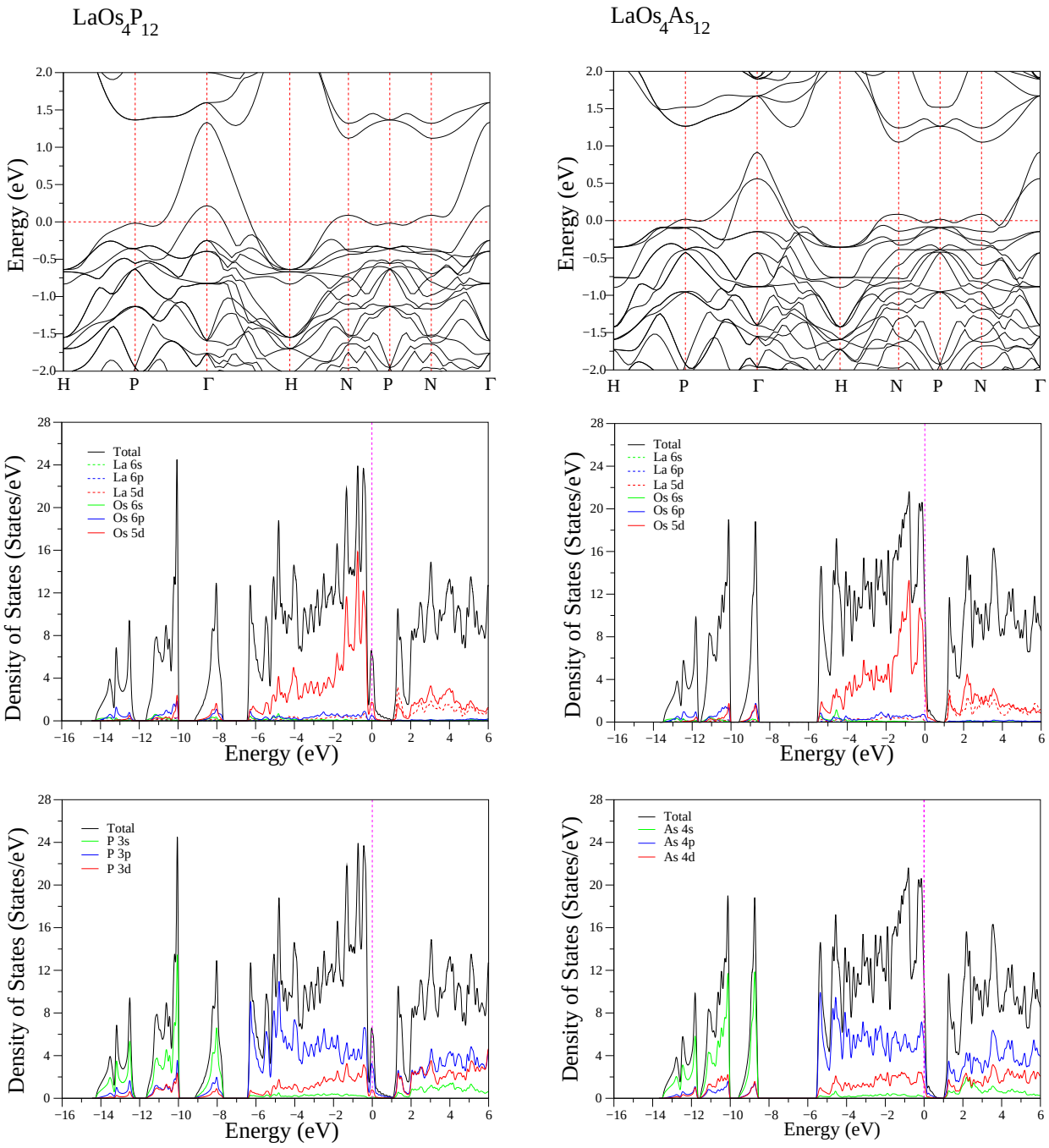

FIG. 3: The electronic band structure and density of states for $LaOs_4P_{12}$ and $LaOs_4As_{12}$. The Fermi level corresponds to 0 eV.

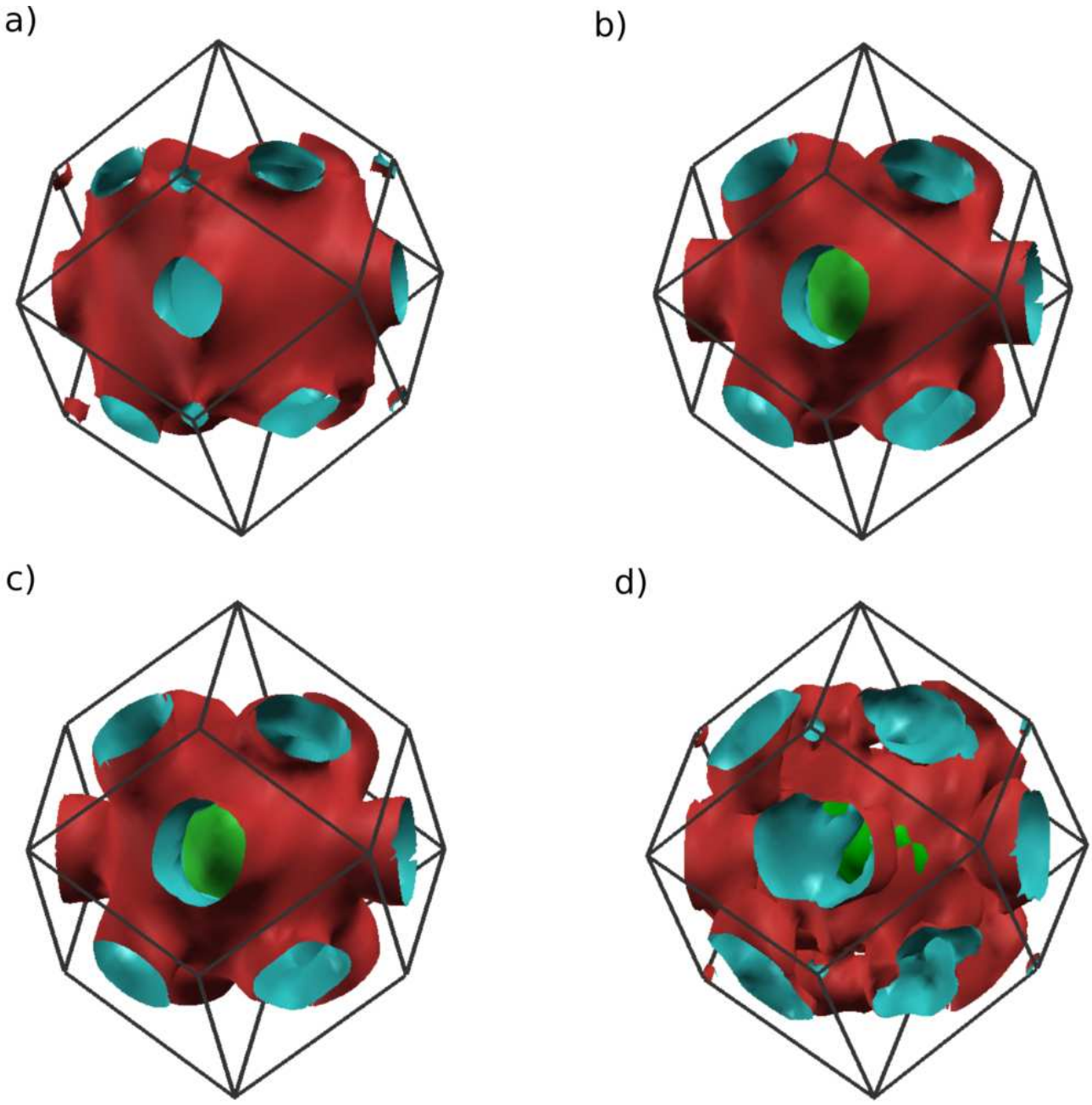

FIG. 4: The calculated Fermi surfaces of a)YRu_4P_{12}, b)YOs_4P_{12},c)$LaOs_4P_{12}$, and d)$LaOs_4As_{12}$.

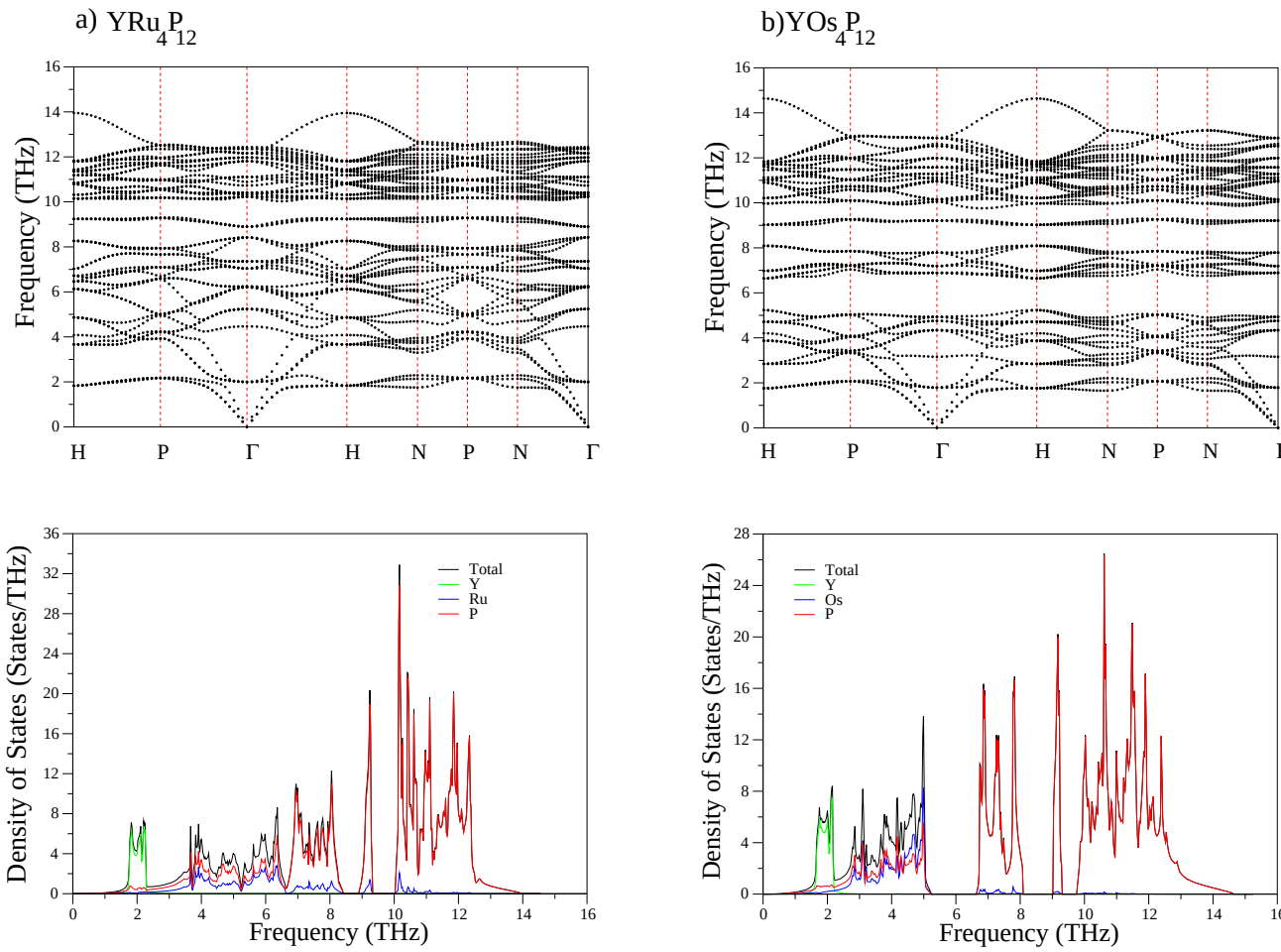

FIG. 5: The phonon dispersion curves and phonon density of states for (a) YRu_4P_{12} and (b) YOs_4P_{12}.

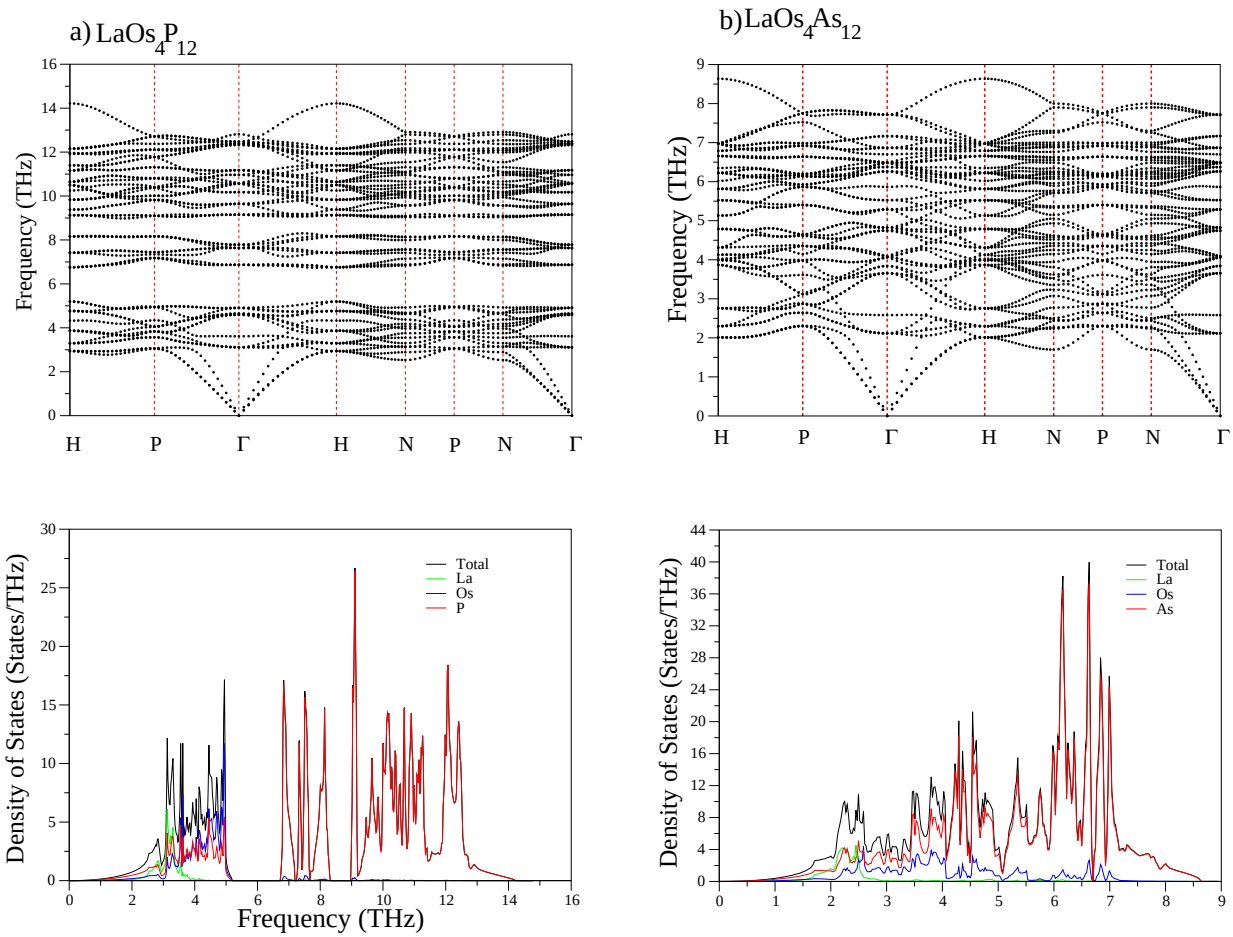

FIG. 6: The phonon dispersion curves and phonon density of states for (a) $LaOs_4P_{12}$ and (b) $LaOs_4As_{12}$.

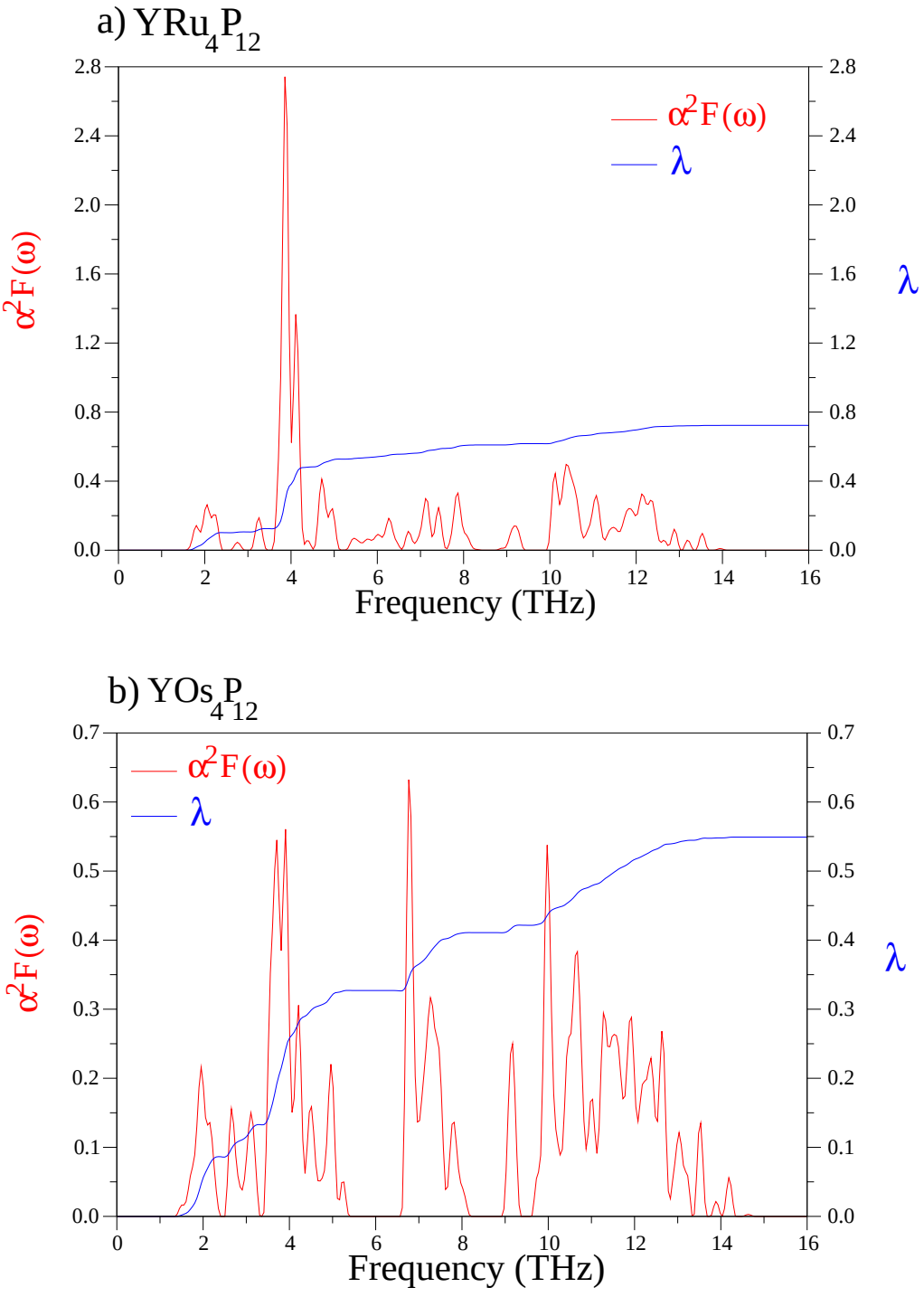

FIG. 7: The calculated electron-phonon spectral function $\alpha^2F(\omega)$ (red line) and the frequency variation of the average electron-phonon coupling parameter λ (blue line) for (a) YRu_4P_{12} and (b) YOs_4P_{12} compounds.

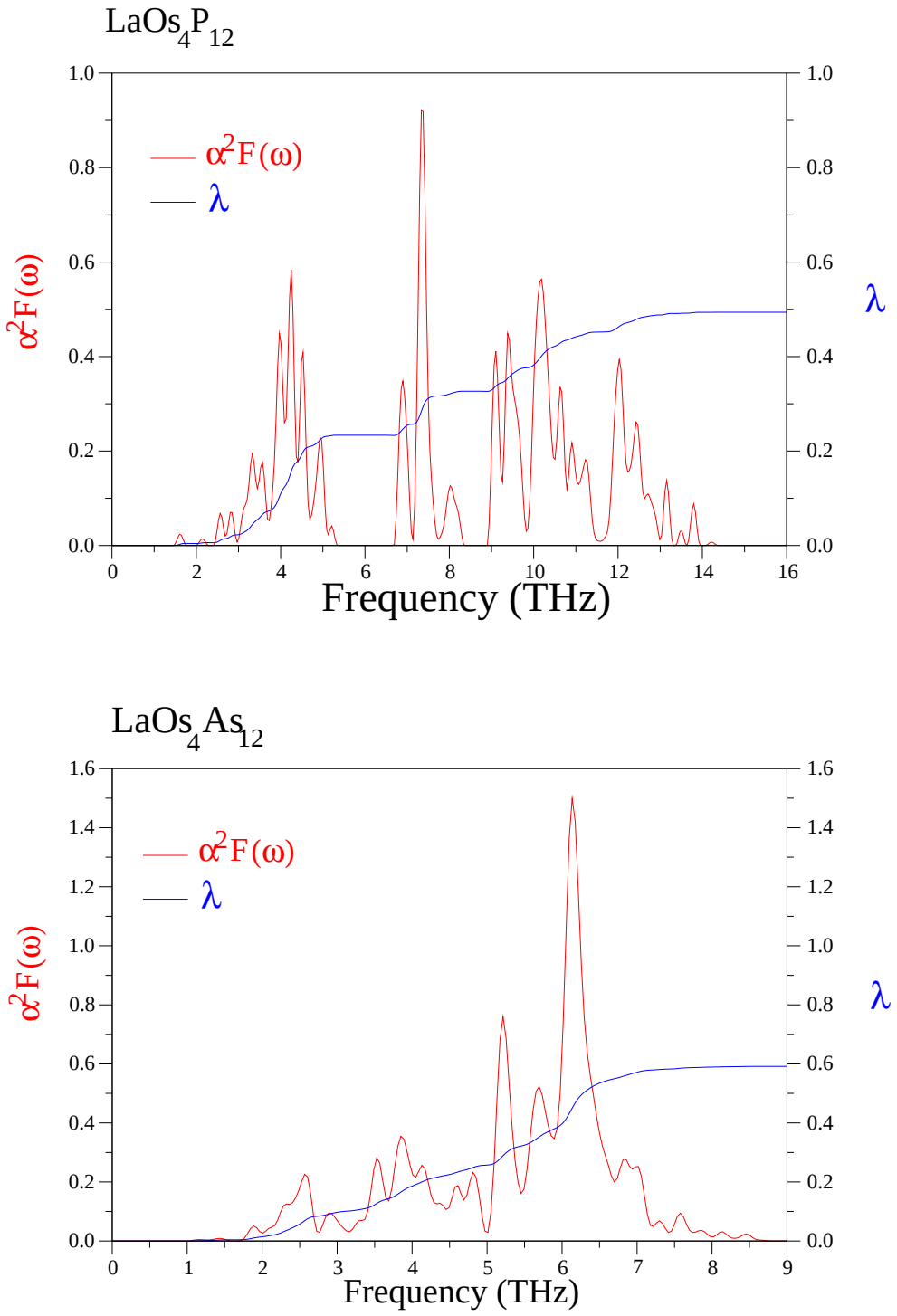

FIG. 8: The calculated electron-phonon spectral function α^2F(ω) (red line) and the frequency variation of the average electron-phonon coupling parameter λ (blue line) for $LaOs_4P_{12}$ and $LaOs_4As_{12}$ compounds.